Redox-Dependent Modulation of Aconitase Activity in Intact Mitochondria†

Anne-Laure Bulteau,§ Masao Ikeda-Saito,‡ and Luke I. Szweda*,§

Department of Physiology and Biophysics, Case Western Reserve University, Cleveland, Ohio 44106-4970, and Institute of Multidisciplinary Research for Advanced Materials, Tohoku University, Katahira, Aoba-ku, Sendai 980-8577, Japan

Received August 5, 2003; Revised Manuscript Received October 21, 2003

ABSTRACT: It has previously been reported that exposure of purified mitochondrial or cytoplasmic aconitase to superoxide ($O_2^{\bullet}$) or hydrogen peroxide (H_2O_2) leads to release of the Fe-α from the enzyme's $[4Fe-4S]^{2+}$ cluster and to inactivation. Nevertheless, little is known regarding the response of aconitase to pro-oxidants within intact mitochondria. In the present study, we provide evidence that aconitase is rapidly inactivated and subsequently reactivated when isolated cardiac mitochondria are treated with H_2O_2. Reactivation of the enzyme is dependent on the presence of the enzyme's substrate, citrate. EPR spectroscopic analysis indicates that enzyme inactivation precedes release of the labile Fe-α from the enzyme's $[4Fe-4S]^{2+}$ cluster. In addition, as judged by isoelectric focusing gel electrophoresis, the relative level of Fe-α release and cluster disassembly does not reflect the magnitude of enzyme inactivation. These observations suggest that some form of posttranslational modification of aconitase other than release of iron is responsible for enzyme inactivation. In support of this conclusion, H_2O_2 does not exert its inhibitory effects by acting directly on the enzyme, rather inactivation appears to result from interaction(s) between aconitase and a mitochondrial membrane component responsive to H_2O_2. Nevertheless, prolonged exposure of mitochondria to steady-state levels of H_2O_2 or $O_2^{\bullet}$ results in disassembly of the $[4Fe-4S]^{2+}$ cluster, carbonylation, and protein degradation. Thus, depending on the pro-oxidant species, the level and duration of the oxidative stress, and the metabolic state of the mitochondria, aconitase may undergo reversible modulation in activity or progress to $[4Fe-4S]^{2+}$ cluster disassembly and proteolytic degradation.

Aconitase belongs to the family of iron−sulfur containing dehydratases whose activities depend on the redox state of the cubane $[4Fe-4S]^{2+}$ cluster. It has been shown that exposure of purified mitochondrial or cytoplasmic aconitase to oxidants, particularly superoxide ($O_2^{\bullet}$) and hydrogen peroxide (H_2O_2), leads to the release of the solvent exposed Fe-α in the ferrous oxidation state and the formation of a $[3Fe-4S]^{1+}$ cluster (*1*−*3*). This process renders the enzyme inactive with respect to interconversion of citrate and isocitrate and has led to the proposal that oxidants play a role in cluster disassembly in vivo (*4*, *5*). Loss in aconitase activity in cells or in biological samples treated with pro-oxidants or isolated from animals undergoing certain pathophysiological processes has therefore been interpreted primarily as a measure of oxidative damage (*5*−*11*). Nevertheless, it has been demonstrated in vitro that reactivation of aconitase can occur upon removal of oxidants and reinsertion of a ferrous ion into the cluster (*12*, *13*). The potential for reversible alterations in aconitase structure and function in response to changes in redox status suggests a potential regulatory role (*5*, *14*, *15*). It is therefore important to investigate the mechanisms of inactivation and the potential for reactivation in more complex experimental models. In addition, studies that distinguish between effects of oxidants on mitochondrial and cytoplasmic aconitase are required.

While active site residues are conserved between the cytoplasmic and the mitochondrial forms of aconitase, these two proteins are capable of carrying out distinct functions (*4*, *16*, *17*). Cytoplasmic aconitase has received considerable attention because loss of its [4Fe−4S] cluster results in the conversion of this enzyme to the iron regulatory protein-1 (IRP1).[1] IRP1 binds to iron-responsive elements (IRE) on either the 5′ or the 3′ untranslated region of a diverse range of mRNAs encoding proteins involved in iron storage and transport (*18*−*20*). Thus, events that control the conversion of cytoplasmic aconitase to IRP1 serve to regulate iron homeostasis (*21*). Mitochondrial aconitase is a Krebs cycle enzyme that catalyzes the reversible interconversion of citrate and isocitrate and plays a critical role in NAD(P)H homeostasis. The mitochondrial electron transport chain is a source of oxygen derived free radicals and pro-oxidants. Production

† This work was supported by Grant 0325305B to A.-L.B. from the American Heart Association, Grant AG-16339 to L.I.S. from the National Institutes of Health, and Grants-in-aid (1214720 and 114380300 to M.I.-S.) from the Ministry of Education, Science, Culture, Sport, and Technology, Japan.

* Correspondence should be addressed to the following author. Telephone: (216) 368-0035. Fax: (216) 368-1693. E mail: Lxs54@po.cwru.edu.

‡ Tohoku University.

§ Case Western Reserve University.

[1] Abbreviations: IRP1, iron regulatory protein 1; EPR, electron paramagnetic resonance; c- and m-aconitase, cytoplasmic and mitochondrial aconitase; DCFDA, 2′-7′-dichlorofluorescein diacetate; DCF, 2′-7′-dichlorofluorescein; MOPS, 4-morpholinopropanesulfonic acid; IRE, iron responsive element; NEM, *N*-ethylmaleimide; PMSF, phenylmethylsulfonyl fluoride; PEG, poly(ethylene glycol); SOD, superoxide dismutase; HET, hydroethidine; E^+, ethidine; IEF, isoelectric focusing; DNPH, 2,4-dinitrophenylhydrazine; DNP, 2,4-dinitrophenylhydrazone.

10.1021/bi0353979 CCC: $25.00
Published on Web 11/26/2003

of these reactive species increases when electron transport slows due to reduced demand for ATP and under conditions where respiratory chain components are altered (*22*−*24*). Loss in mitochondrial aconitase activity in response to pro-oxidants may therefore limit the further production of oxidant species by decreasing the production of NADH, and thus, reducing equivalents for electron transport, thereby serving as a protective response to oxidative stress (*5*, *9*, *14*, *15*, *25*). However, oxidatively inactivated mitochondrial aconitase has recently been shown to be readily degraded by purified Lon, an ATP-dependent mitochondrial protease (*26*). Thus, the response of aconitase to pro-oxidants has the potential to progress from reversible alterations in activity to enhanced proteolytic degradation.

A variety of antioxidants, regulatory factors, and metabolic conditions exist within intact mitochondria that contribute to a dynamic response to oxidative stress. It is therefore important to characterize and evaluate the response of aconitase to pro-oxidants within intact mitochondria. To date, treatment of mitochondria with $O_2^{\bullet}$ or H_2O_2 has been shown to result in inactivation of aconitase and release of iron from the enzyme's $[4Fe-4S]^{2+}$ cluster (*3*, *27*). In the present study, mitochondria isolated from rat heart were exposed to H_2O_2 and $O_2^{\bullet}$ in order to (1) assess the potential for reversible alterations in aconitase activity; (2) evaluate mechanisms by which aconitase structure and function are altered; and (3) investigate conditions under which aconitase is degraded. We provide evidence for reversible modulation of aconitase activity in response to H_2O_2. The results indicate a novel mechanism of inactivation in which aconitase undergoes loss in activity not as a result of direct interaction with H_2O_2 but rather with a mitochondrial membrane component responsive to H_2O_2. The presence of the enzyme's substrate, citrate, and the duration of the oxidant exposure determine the progression from reversible redox modulation of aconitase activity to irreversible oxidative damage. Loss in aconitase activity has been observed during certain physiological and pathophysiological processes associated with increased generation of oxygen radicals (*6*, *7*, *9*). The results of the present study provide new insight into events that may contribute to loss in activity and suggest potential physiological implications.

MATERIALS AND METHODS

Isolation of Subsarcolemmal Mitochondria from Rat Heart. Male Sprague−Dawley rats (Harlan, 250−300 g) were anesthetized with sodium pentobarbital and decapitated. Hearts were removed and immediately rinsed in ice-cold buffer A (210 mM mannitol, 5.0 mM MOPS, 70 mM sucrose, 1.0 mM EDTA, pH 7.4). Hearts (0.9−1.1 g) were then minced and homogenized in 20 mL of buffer A with a Polytron homogenizer (low setting, 2 s). The homogenate was centrifuged at 500*g* for 5 min, and the supernatant was filtered through cheesecloth. The mitochondrial pellet was obtained upon centrifugation of the supernatant at 10 000*g* for 10 min. After two rinses with ice-cold buffer, the mitochondria were resuspended into buffer A prepared without EDTA to a final concentration of 40.0 mg/mL. Protein determinations were made using the BCA method (Pierce), using bovine serum albumin as a standard. For matrix preparations, mitochondria were ruptured by sonication at maximum intensity, and the matrix fraction was separated by centrifugation at 100 000*g* for 1 h (4 °C) as previously described (*28*).

Incubation of Intact Mitochondria with H_2O_2. Mitochondria were diluted to 0.25 mg/mL in buffer B (125 mM KCl and 5.0 mM KH_2PO_4, pH 7.25) in the absence or presence of exogenously added citrate, α-ketoglutarate, and/or pyruvate/malate. Mitochondria were then incubated for 2.0 min followed by addition of 100 μM H_2O_2. All incubations were performed at room temperature.

Assay of Aconitase. Aconitase activity was evaluated after exposure of cardiac mitochondria to various experimental conditions. Mitochondria were diluted to 0.05 mg/mL in 25 mM KH_2PO_4, pH 7.25, containing 0.05% Triton X-100. Aconitase activity was assayed as the rate of NADP reduction (340 nm, $\epsilon = 6200\ M^{-1}\ cm^{-1}$) by isocitrate dehydrogenase upon addition of 1.0 mM sodium citrate, 0.6 mM $MnCl_2$ (a cofactor of isocitrate dehydrogenase), 0.2 mM NADP, and 1.0 U/mL isocitrate dehydrogenase to solubilized mitochondria (0.05 mg/mL mitochondrial protein). Isocitrate dehydrogenase (Sigma) was exchanged into a buffer composed of 25 mM KH_2PO_4, pH 7.25 by gel filtration (PD-10 column, Amersham-Pharmacia Biotech) prior to incubations. Use of oxalomalate (2.0 mM), a competitive inhibitor of aconitase, ensured the specificity of the assay.

Triton x-100 solubilization of mitochondria prevented continued inactivation of aconitase during enzyme analysis. At the end of each experimental protocol, mitochondria are diluted 1:5 (for experiments where 0.25 mg/mL of mitochondria were utilized) or 1:600 (for experiments where 30 mg/mL of mitochondria were utilized for EPR analysis) in assay buffer containing 0.05% Triton x-100. The enzyme was then assayed within 30 s. Importantly, Triton x-100 solubilization of the mitochondria retards the rate of aconitase inactivation such that no inactivation is observed over this time frame when control mitochondria are first solubilized and then H_2O_2 is added. Additionally, there is no difference in the level of inactivation or reactivation when aconitase is assayed 30 s or 2 min after solubilization of the mitochondria.

Enzymatic Generation of Extramitochondrial H_2O_2 and $O_2^{\bullet}$ at Steady-State Levels. The enzymatic oxidation of glucose catalyzed by glucose oxidase yields H_2O_2. Under conditions of substrate saturation (both glucose and dioxygen), the rate of H_2O_2 generation is described by the equation $dH_2O_2/dt = kGO$ (rate constant of glucose oxidase). H_2O_2 degradation from the mitochondria depends only on the H_2O_2 concentration and follows first-order kinetics (*29*). Thus, at steady-state conditions, the concentration of H_2O_2 is determined by the ratio of *k*GO/*k*(mitochondria). On the basis of these considerations, the amount of glucose oxidase required to generate a steady-state level of 100 μM H_2O_2 (maintained for 30 min) can be calculated. In typical experiments, mitochondria were diluted to 0.25 mg/mL in buffer B in the presence of 2 mM sodium citrate and incubated with 5 mM glucose and glucose oxidase (5.0 U/mL). As necessary, the production of H_2O_2 by glucose/glucose oxidase was quenched by addition of catalase (0.25 mg/mL).

$O_2^{\bullet}$ was generated utilizing the enzyme xanthine oxidase and substrate xanthine. Because H_2O_2 can be produced from superoxide dismutation, catalase was added to the reaction mixture. Mitochondria were diluted to 0.25 mg/mL in buffer B in the presence of 2.0 mM sodium citrate. Two minutes after substrate addition, mitochondria were incubated with

0.5 mM xanthine and catalase (500 U/mL) in the presence or absence of 25.0 mU of xanthine oxidase. Rates of $O_2^{\bullet}$ production by xanthine/xanthine oxidase were estimated by following the initial rate of cytochrome c^{3+} reduction at 550 nm under mock exposure conditions with 10 μM cytochrome c^{3+} and without mitochondria. Under these experimental conditions, $O_2^{\bullet}$ was produced at a relatively high rate: 2.0 nmol min^{-1} mL^{-1}. To quench $O_2^{\bullet}$ generation, superoxide dismutase (200 U/mL) was added.

Assay of H_2O_2 and $O_2^{\bullet}$. (A) Determination of Extra-Mitochondrial H_2O_2 Concentrations. Mitochondria were diluted to 0.25 mg/mL in buffer B in the presence of 2.0 mM sodium citrate and treated with a bolus or a steady-state level of H_2O_2. At appropriate time points, an aliquot of 20 μL was transferred to an assay mixture containing horseradish peroxidase (1.0 U/mL) and 500 μM homovanillic acid (3-metoxy-4-hydroxyphenylacetic) in 25 mM KH_2PO_4, pH 7.25 (total volume = 2 mL). The fluorescence of the sample was measured using a spectrofluorometer (Shimadzu) at excitation/emission wavelengths of 320/425 nm. A standard curve was generated using various concentrations of H_2O_2.

(B) Fluorometric Assay for Monitoring Intramitochondrial H_2O_2 and $O_2^{\bullet}$ Concentrations. Mitochondria were diluted to 0.25 mg/mL in buffer B in the presence of 2.0 mM sodium citrate and treated with rotenone or xanthine and xanthine oxidase. At appropriate time points, an aliquot was taken and transferred to an assay mixture containing 50 mM KH_2PO_4, pH 7.6 and 1.0 μM DCFDA in a final volume of 0.15 mL. Fluorescence readings (excitation at 485 nm and emission at 522 nm) were followed for 5 min. The quantitative evaluation of DCF fluorescence was undertaken utilizing serial dilutions of commercial DCF solution. All measurements with DCFDA were compared with blanks run in parallel (*30*). Hydroethidine (HET) oxidation to fluorescent ethidine (E^+) was used as a measure of $O_2^{\bullet}$. Mitochondria were diluted to 0.2 mg/mL in buffer B and incubated with 3.0 μM HET for 30 min and centrifuged for 5 min at 15 000 rpm. At appropriate time points, an aliquot of the solution was transferred to an assay mixture containing 50 mM KH_2PO_4, pH 7.6 (final volume = 0.15 mL). Fluorescence readings (excitation at 470 nm and emission at 590 nm) were taken for 10 min (*31*).

Electron Paramagnetic Resonance (EPR) Spectroscopy. Cardiac mitochondria (30 mg/mL) were exposed to various experimental conditions, placed in quartz EPR tubes, and frozen by immersion in liquid nitrogen. EPR spectra were recorded by a Bruker ESP300 spectrometer operating at 9.45 GHz with 10 G field modulation at 100 kHz. Measurements were carried out at 10 K by use of an Oxford liquid He flow cryostat. The microwave frequency was monitored by a frequency counter (HP-5350), and the magnetic field strength was determined by an NMR Gaussmeter (Brucker ER-035M). Each spectrum represents an average of 32 scans. Purified aconitase from beef heart and mitochondrial matrix was utilized to assign spectral peak(s) specific to aconitase. Utilizing highly purified aconitase in the $[3Fe-4S]^{1+}$ form (a gift from M. Claire Kennedy), a standard curve for quantification of the EPR data was constructed. The content of aconitase present in mitochondria relative to purified protein was standardized based on activity measurements between untreated mitochondria and purified aconitase reactivated upon anaerobic incubation with 10 mM DTT and 0.5 mM $FeSO_4$ in 100 mM Tris, pH 7.4 for 30 min at 0 °C.

Isoelectric Focusing (IEF) Gel Electrophoresis. Following exposure of cardiac mitochondria to various experimental conditions, mitochondria were diluted into 25 mM KH_2PO_4, pH 7.25 containing 0.05% Triton X-100 and resolved by IEF gel electrophoresis (10 μg of protein per lane) and Western blot analysis utilizing polyclonal antibody specific to aconitase. Isoelectric focusing was performed using the Criterion IEF system (BioRad).

Western Blot Analysis. Prior to analysis, mitochondrial extracts were incubated in Laemmli sample buffer for 5.0 min at 100 °C. Mitochondrial proteins (20 μg/lane) were resolved on a 12% SDS−PAGE gel and electrotransferred onto a Hybond nitrocellulose membrane (Amersham Pharmacia Biotech). Blots were then probed using polyclonal antibody specific to aconitase. Primary antibody binding was visualized utilizing peroxidase-conjugated secondary antibody and an appropriate chemiluminescent substrate (Supersignal West from Pierce).

Aconitase Immunopurification. A polyclonal antibody against aconitase targeted to residues 767−780 of the carboxyl terminus of human mitochondrial aconitase was produced (rabbit host). After exposure of cardiac mitochondria to various experimental conditions, mitochondria were diluted to 1.0 mg/mL in 25 mM KH_2PO_4, pH 7.25, containing 0.05% Triton X-100. Mitochondrial extracts (500 μg in 0.1 mL) were incubated with 10 μL of anti-aconitase polyclonal antibody at 4 °C for 1 h. The mixture was then treated with 50 μL of protein G-Sepharose and incubated for 16 h (4 °C). The mixture was centrifuged at 1000*g* for 5 min, and the beads were washed three times with phosphate-buffered saline (PBS), pH 7.6 containing 1% NP-40 and resuspended in gel-loading buffer containing SDS but without reductant. The samples were incubated in gel-loading buffer at room temperature (10 min) prior to gel electrophoresis/Western blot analysis.

Detection of Carbonylated Aconitase. To detect oxidized aconitase, we utilized the Oxyblot kit (Intergen). This assay is based on the derivatization of carbonyl groups with 2,4-dinitrophenylhydrazine (DNPH). Western blot analyses were performed utilizing 2.0 μg of immunopurified aconitase per lane and primary antibody against dinitrophenylhydrazone (DNP).

RESULTS

Treatment of Intact Mitochondria with H_2O_2: Effect on Aconitase Activity. Aconitase loses activity upon addition of H_2O_2 to cardiac mitochondria. Subsequent reactivation is dependent on the presence of citrate. As shown in Figure 1A, treatment of mitochondria with 100 μM H_2O_2 in the absence of added Krebs cycle intermediates led to rapid inactivation of aconitase with no recovery in activity evident over a 30 min incubation period. In contrast, in the presence of the enzyme's substrate citrate, aconitase was rapidly inactivated followed by a time-dependent recovery in activity to approximately 80% of the control values. Recovery of aconitase activity was slowed when mitochondria were solubilized following inactivation indicating that interactions between aconitase and certain mitochondrial components are important for enzyme reactivation. Incubation of mitochon-

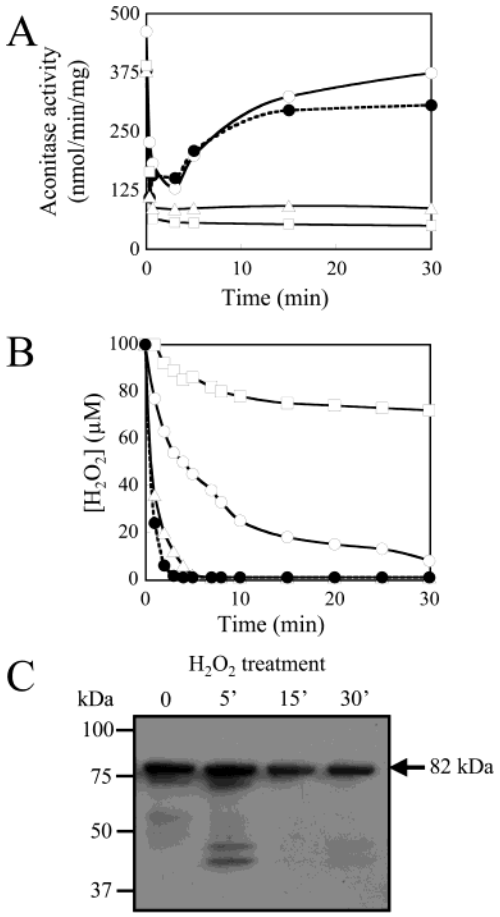

FIGURE 1: Inactivation and reactivation of aconitase in intact mitochondria treated with H_2O_2. Intact mitochondria (0.25 mg/mL) were incubated with 100 μM H_2O_2 in the presence of 2.0 mM citrate (○), 15 mM α-ketoglutarate (△), 10 mM pyruvate, and 2.5 mM malate (●) or in the absence of substrate (□) at 25 °C. Panel A: fractional alterations in aconitase activity in response to H_2O_2. At indicated times, mitochondria were disrupted, and aconitase activity was determined as described in Materials and Methods. Panel B: mitochondrial consumption of exogenously added H_2O_2. At indicated times, the concentration of H_2O_2 in the media was monitored as the increase in *p*-hydroxyphenylacetate fluorescence (excitation and emission wavelengths of 320 and 425 nm, respectively) upon the addition of horseradish peroxidase as described in Materials and Methods. Panel C: H_2O_2-induced proteolysis of aconitase. Intact mitochondria (0.25 mg/mL) were incubated with 100 μM H_2O_2 in the presence of 2.0 mM citrate. At indicated times, mitochondria were disrupted, and mitochondrial proteins (10 μg/lane) were resolved by SDS−PAGE (12% gels) and analyzed by Western blot analysis utilizing polyclonal antibodies raised against aconitase as described in Materials and Methods. The blot depicted is representative of three separate experiments.

dria with citrate resulted in the rapid removal of H_2O_2 relative to the rate observed in the absence of substrate (Figure 1B). Nevertheless, no recovery of aconitase activity was evident in mitochondria incubated with α-ketoglutarate (Figure 1A), despite the fact that H_2O_2 was removed at a faster rate than in the presence of citrate (Figure 1B). α-Ketoglutarate can be converted to citrate by isocitrate dehydrogenase (*32*). However, due to thermodynamic constraints, this is likely to result in significantly lower concentrations of intramitochondrial citrate relative to those arising from direct addition of citrate. It therefore appears that citrate contributes to the eventual recovery of aconitase activity. In support of this conclusion, when mitochondria were exposed to H_2O_2 in the presence of pyruvate and malate, thus enabling the formation of citrate, reactivation of aconitase was observed as was the rapid disappearance of H_2O_2 (Figure 1A,B). Additionally, when isocitrate was added to mitochondria following 2 min of H_2O_2 exposure in the absence of substrate, aconitase activity was recovered (results not shown). Thus, recovery of enzyme activity may be facilitated by binding of substrate or product to the enzyme's active site. Comparison of Figure 1A,B indicates that recovery of aconitase activity in the presence of citrate began when approximately 50% of the initial H_2O_2 had been consumed. These results indicate a dynamic response of aconitase activity to changes in the level of H_2O_2. As judged by Western blot analysis utilizing antibodies specific for aconitase, fragments of aconitase were generated as a consequence of H_2O_2 treatment of mitochondria in the presence of citrate. These fragments were not observed at longer incubation periods when enzyme activity had recovered indicating partial degradation of inactive aconitase. In addition, a decrease in the level of full-length protein was evident (Figure 1C). These results are consistent with an oxidant-induced increase in proteolytic susceptibility of aconitase and provide an explanation for the lack of full recovery in activity even in the presence of citrate (Figure 1A).

Effect of H_2O_2 on Aconitase [4Fe−4S] Cluster. It has previously been shown that aconitase can be inactivated as a result of pro-oxidant-induced release of a labile iron from the [4Fe−4S] cluster of the enzyme ($[4Fe-4S]^{2+} \rightarrow [3Fe-4S]^{1+}$). This has been demonstrated using primarily purified preparations of cytoplasmic and mitochondrial aconitase exposed to superoxide anion and/or H_2O_2 (*1*−*3*). To investigate whether this mechanism is responsible for enzyme inactivation in intact mitochondria, mitochondria were treated with H_2O_2 in the presence of citrate and solubilized at various times of incubation. Mitochondrial proteins were then resolved by nondenaturing isoelectric focusing gel electrophoresis and probed utilizing Western blot analysis with an antibody specific for aconitase. The pI values for $[4Fe-4S]^{2+}$-, $[3Fe-4S]^{1+}$-, and apo-enzyme are 7.8, 7.5, and 8.0, respectively. Despite the fact that greater than 60% loss in aconitase activity was observed within the first 40 s (Figure 1A), no statistically significant change in intensity of antibody binding to aconitase migrating with an isoelectric point consistent with the $[4Fe-4S]^{2+}$ cluster relative to total binding (Figure 2A) was observed as judged by densitometric analysis ($n = 4$). In addition, aconitase in the $[3Fe-4S]^{1+}$ and apo forms did not show statistically significant changes in levels as a function of time of exposure and did not represent greater than 20% of the total protein as determined by antibody binding (Figure 2A). These data support the premise that release of the Fe-α from the $[4Fe-4S]^{2+}$ cluster is not the primary event responsible for H_2O_2-induced inactivation of aconitase in intact mitochondria. Alternatively, posttranslational modifications distinct from release of Fe may alter the isoelectric focusing pattern of aconitase containing the $[3Fe-4S]^{1+}$ cluster.

Because of the semiquantitative nature of IEF Western blot analysis, it was necessary to obtain more quantitative information using EPR spectroscopy. To observe aconitase utilizing EPR spectroscopy, higher concentrations of mitochondria, and thus, H_2O_2 (30 mg/mL treated with 2.0 mM H_2O_2) were required than in the experiments depicted in Figures 1 and 2A. Nevertheless, while these conditions

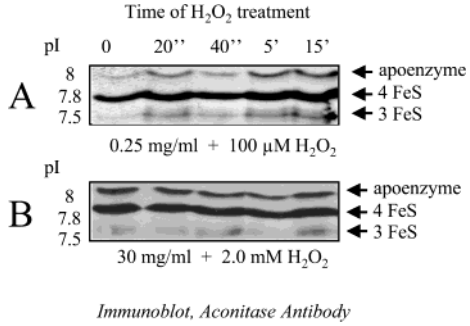

FIGURE 2: Alterations in the relative distribution of various forms of aconitase in response to H_2O_2. Intact mitochondria ((A) 0.25 mg/mL or (B) 30 mg/mL) were incubated with ((A) 100 μM or (B) 2.0 mM) H_2O_2 in the presence of 2.0 mM citrate at 25 °C. At indicated times, mitochondria were disrupted and analyzed by nondenaturing IEF gel electrophoresis (10 μg/lane) and Western blot analysis utilizing polyclonal antibodies raised against aconitase as described in Materials and Methods.

A

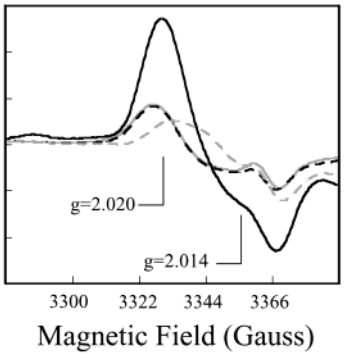

B

Time	0	20"	40"	2'	5'	10'	15'
% Initial Aconitase activity	100	24	53	67	76	78	83
% Aconitase as [3Fe-4S] cluster	0	4	15	13	12	4	4

FIGURE 3: Time-dependent inactivation/reactivation of aconitase and appearance and disappearance of EPR detectable $[3Fe-4S]^{1+}$ cluster in response to H_2O_2 treatment in the presence of citrate. Intact mitochondria (30 mg/mL due to protein requirement for EPR analysis) were incubated with 2.0 mM H_2O_2 in the presence of 2.0 mM citrate. At indicated periods of time, mitochondria were diluted and solubilized for assay of aconitase activity or quick-frozen and analyzed by EPR spectroscopy as described in Materials and Methods. (A) Representative EPR spectra at 20 s (solid gray line), 40 s (solid black line), and 15 min (dashed black line) following H_2O_2 addition. To obtain a control EPR spectrum (dashed gray line), mitochondria were incubated without H_2O_2 in the presence of 2.0 mM citrate prior to analysis. (B) % initial aconitase activity and % aconitase containing $[3Fe-4S]^{1+}$ cluster. Quantification of the EPR data was accomplished using purified aconitase in the $[3Fe-4S]^{1+}$ form as a standard as described in Materials and Methods.

resulted in a change in the time course of inactivation and reactivation of aconitase (Figure 3B), IEF Western blot analysis indicates that no statistically significant change in intensity of antibody binding to aconitase migrating with an isoelectric point consistent with the $[4Fe-4S]^{2+}$ cluster was observed relative to total binding (Figure 2B). Thus, these observations demonstrate a similar response of aconitase to H_2O_2 at the two different protein and H_2O_2 concentrations. EPR spectroscopy was therefore employed to analyze mitochondria exposed to H_2O_2 for varying periods of time.

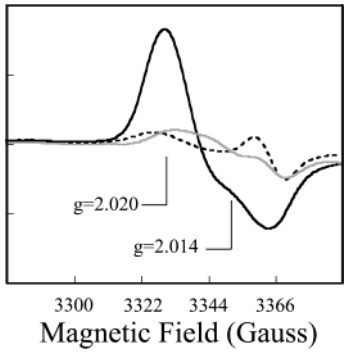

FIGURE 4: EPR spectra of the $[3Fe-4S]^{1+}$ cluster of aconitase in response to H_2O_2 treatment in the presence or absence of α-ketoglutarate. Intact mitochondria (30 mg/mL) were incubated with 2.0 mM H_2O_2 in the presence (dashed black line) or absence (solid black line) of 15.0 mM α-ketoglutarate for 5.0 min. Samples were then quick-frozen and analyzed by EPR spectroscopy as described in Materials and Methods. To obtain a control EPR spectrum (solid gray line), mitochondria were incubated without H_2O_2 in the presence of 15.0 mM α-ketoglutarate prior to analysis.

Aconitase containing the $[4Fe-4S]^{2+}$ cluster is EPR silent. In contrast, the $[3Fe-4S]^{1+}$ cluster of aconitase, formed upon release of the labile Fe-α under oxidizing conditions, is characterized as a peak at $g = 2.02$ with a shoulder at $g = 2.014$ in the EPR spectrum (10 K) (*3*, *4*, *13*). As shown in Figure 3A, a peak corresponding to aconitase containing the $[3Fe-4S]^{1+}$ cluster was observed upon treatment of mitochondria with H_2O_2 in the presence of citrate. The time-dependent increase in this peak did not, however, reflect the degree of enzyme inactivation. Under the conditions of these experiments, aconitase activity was 24% that of control at 20 s after H_2O_2 addition (Figure 3B). Nevertheless, maximum EPR signal intensity corresponding to the $[3Fe-4S]^{1+}$ cluster of aconitase was not observed until 40 s, despite the fact that the enzyme activity had begun to recover (53% of control) (Figure 3B). This was followed by a time-dependent decline of the signal intensity to control values upon further reactivation of aconitase (Figure 3A,B). Utilizing highly purified aconitase in the $[3Fe-4S]^{1+}$ form as a standard for quantification of the EPR data, conversion to the $[3Fe-4S]^{1+}$ form of the protein upon treatment of mitochondria with H_2O_2 represents only 15% of the total aconitase at maximum peak intensity (40 s). Because enzyme inactivation precedes the appearance of an EPR signal corresponding to the $[3Fe-4S]^{1+}$ cluster and a small percentage of the $[4Fe-4S]^{2+}$ cluster is converted to $[3Fe-4S]^{1+}$ relative to the loss in activity, it is likely that some other form of posttranslational modification of the enzyme is responsible for loss of enzyme activity.

Despite 75% inactivation of aconitase when mitochondria (30 mg/mL) were incubated with H_2O_2 (2.0 mM) for 5 min in the presence of α-ketoglutarate, the appearance of the $[3Fe-4S]^{1+}$ cluster was not observed as judged by EPR spectroscopy (Figure 4). Full disassembly of the $[4Fe-4S]$ cluster is unlikely. Following inactivation of aconitase and H_2O_2 consumption in mitochondria incubated with α-ketoglutarate, addition of citrate resulted in rapid enzyme reactivation (not shown). These results indicate that full cluster disassembly has not occurred given that reactivation was evident within a time frame shorter than would be expected for cluster reassembly (*33*−*35*). In addition, in the absence of respiratory substrate, where the presence of H_2O_2

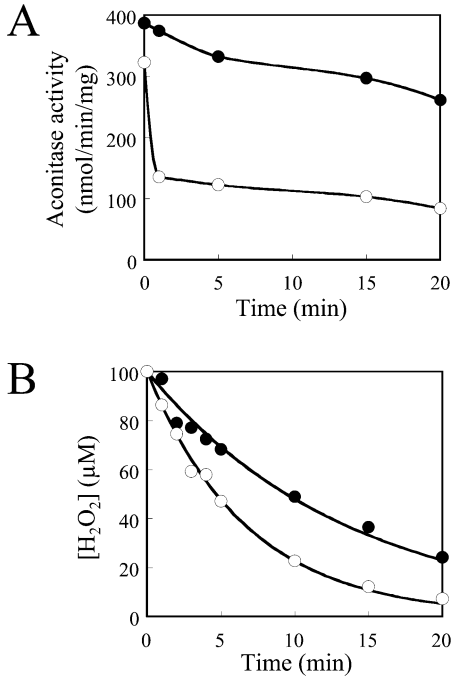

FIGURE 5: Conditions required for aconitase inactivation. Panel A: effect of H_2O_2 on the activity of aconitase in mitochondrial matrix. Matrix and membrane subfractions were prepared as described in Materials and Methods. Matrix alone (●) or in the presence of 1 equiv of mitochondrial membrane fraction (○) was incubated for 30 min at 25 °C and treated with 100 μM H_2O_2. At times indicated on the abscissa, samples were assayed for aconitase activity. Panel B: consumption of exogenously added H_2O_2 by mitochondrial subfractions. Matrix alone (●) or in the presence of 1 equiv of mitochondrial membrane fraction (○) was incubated for 30 min at 25 °C and treated with 100 μM H_2O_2. At times indicated on the abscissa, the concentration of H_2O_2 remaining was evaluated as described in Materials and Methods.

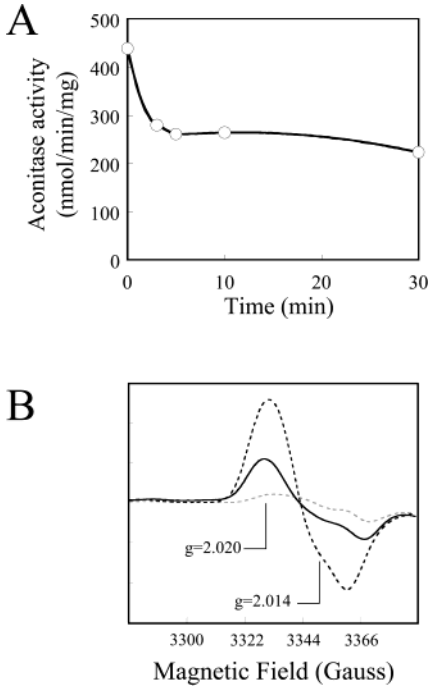

FIGURE 6: Rotenone-mediated inactivation of mitochondrial aconitase. Panel A: effect of rotenone on aconitase activity. Intact mitochondria (0.25 mg/mL) were incubated with 40 μM rotenone in the presence of 2.0 mM citrate at 25 °C (○). At indicated times, mitochondria were disrupted, and aconitase activity was determined as described in Materials and Methods. Panel B: comparison of EPR detectable $[3Fe-4S]^{1+}$ cluster in response to rotenone vs H_2O_2 treatment. Intact mitochondria (30 mg/mL) were incubated (25 °C) with (a) 40 μM rotenone in the presence of 2.0 mM citrate for 30 min (dashed black line); (b) 2.0 mM H_2O_2 in the presence of 2.0 mM citrate for 40 s (solid black line); or (c) 2.0 mM citrate in the absence of rotenone and H_2O_2 (dashed gray line). Samples were then quick-frozen and analyzed by EPR spectroscopy as described in Materials and Methods.

persists and approximately 70% of initial activity has been lost within 5 min, an EPR signal corresponding to the $[3Fe-4S]^{1+}$ cluster of aconitase was observed (Figure 4). Finally, IEF gel electrophoresis/Western blot analysis did not reveal a significant change in the band corresponding to the $[4Fe-4S]^{2+}$ form of the enzyme (not shown). Given the rapid consumption of H_2O_2 in mitochondria respiring with α-ketoglutarate, a reducing environment would be rapidly restored. Lack of EPR observable $[3Fe-4S]^{1+}$ cluster is therefore consistent with posttranslational modification resulting in enzyme inactivation with no subsequent release of labile Fe-α and/or release of labile Fe-α followed by rapid reduction of the $[3Fe-4S]^{1+}$ cluster to EPR silent $[3Fe-4S]^{0}$ (*4*, *13*, *36*). Citrate is therefore required for reversal of posttranslational modification and/or Fe-α reinsertion.

Requirements for H_2O_2-Induced Aconitase Inactivation. Mitochondria were subfractionated to explore components required for H_2O_2-induced inactivation. Mitochondrial matrix preparations containing aconitase but devoid of mitochondrial inner- and outermembrane were treated with 100 μM H_2O_2 in the absence of citrate. As shown in Figure 5A, this resulted in slow inactivation of aconitase relative to that observed for intact mitochondria (Figure 1A). In contrast, addition of the mitochondrial membrane fraction to the matrix preparation resulted in rapid inactivation of aconitase upon addition of H_2O_2 (Figure 5A). The difference in the rate of inactivation cannot be explained by a difference in the rate of removal of H_2O_2. In fact, H_2O_2 was consumed at a greater rate in the presence of the membrane fraction (Figure 5B). Enhancement in the rate of aconitase inactivation by the membrane fraction required preincubation with matrix components, reaching optimum at 15 and 30 min under the conditions of the experiment. These results suggest the requirement for interactions between membrane and matrix components. The addition of deferoxamine, an iron chelator, or dimethylthiourea, an oxygen radical scavenger, had no effect on the rate or extent of inactivation indicating that inactivation is unlikely the result of formation of a more potent oxidant. In addition, heating the membrane fraction (100 °C for 3 min) abolished its ability to promote aconitase inactivation. These results strongly indicate that H_2O_2-induced loss of aconitase activity in intact mitochondria is largely mediated by a membrane component and not by direct interaction of H_2O_2 with the enzyme.

Rotenone-Induced Inactivation of Aconitase. In an effort to determine whether different pro-oxidants inactivate aconitase by distinct mechanisms, mitochondria were incubated with rotenone in the presence of citrate. Treatment of mitochondria with rotenone (40 μM), an inhibitor of complex I, resulted in endogenous production of $O_2^{\bullet-}$ (870 pmol/min/mg) and H_2O_2 (3.84 pmol/min/mg). Under these conditions, a 40% decline in enzyme activity occurred within the first 2 min (Figure 6A). This was followed by relatively little further loss in activity indicative of oxidant-induced reduction in NADH production, electron transport, and thus $O_2^{\bullet}$ genera-

tion. Preloading the mitochondria with PEG-SOD prevented inactivation of aconitase indicating that the species responsible for inactivation is $O_2^{\bullet}$ (not shown). Analysis by EPR spectroscopy demonstrated a signal characteristic of the $[3Fe-4S]^{1+}$ cluster of aconitase consistent with release of the labile iron Fe from the [4Fe−4S] cluster (Figure 6B). Rotenone induced a 46% decline in aconitase activity under the conditions utilized for EPR analysis. The intensity of the EPR signal corresponding to the $[3Fe-4S]^{1+}$ cluster was 2.5-fold greater than the maximum signal intensity observed when mitochondria were treated with 2.0 mM H_2O_2 in the presence of citrate (Figure 6B). The difference in the level of the EPR detectable $[3Fe-4S]^{1+}$ cluster despite similar levels of inactivation provides further support for the conclusion that H_2O_2 induces a posttranslational modification of aconitase other than release of iron that is largely responsible for loss of enzyme activity. In contrast to H_2O_2 (Figure 5A), treatment of mitochondrial matrix components in the absence of the membrane fraction with an $O_2^{\bullet}$ generating system (xanthine/xanthine oxidase) resulted in rapid inactivation of aconitase (not shown). It is therefore apparent that different pro-oxidants act through distinct mechanisms of inactivation.

Effect of Steady-State Production of H_2O_2 and Superoxide Anion ($O_2^{\bullet}$) on Aconitase Activity, [4Fe−4S] Cluster Disassembly, and Proteolytic Degradation. To further explore aconitase inactivation and the potential for [4Fe−4S] cluster disassembly and protein degradation, mitochondria were exposed to a steady-state concentration of H_2O_2 or $O_2^{\bullet}$. With appropriate amounts of glucose, glucose oxidase, and catalase, production and consumption of H_2O_2 was maintained at a concentration of 100 μM (Figure 7A). To produce $O_2^{\bullet}$ at a constant rate (900 pmol/min/mg as measured within the mitochondria) comparable to that for rotenone treated mitochondria, the $O_2^{\bullet}$ generating system xanthine/xanthine oxidase was utilized (Figure 7B). Both pro-oxidants lead to inactivation of aconitase, an effect that was partially inhibited by the presence of citrate. Citrate reduced the initial rate of $O_2^{\bullet}$-induced inactivation but did not exert a similar effect with the pro-oxidant H_2O_2 (Figure 7A,B). In contrast to bolus addition of H_2O_2 (Figures 3B and 4) or rotenone-induced production of $O_2^{\bullet}$ (Figure 6B), the aconitase $[3Fe-4S]^{1+}$ cluster was not observed by EPR spectroscopic analysis despite a 75% reduction in enzyme activity after mitochondria (30 mg/mL) were exposed to 10 min of steady-state production of H_2O_2 and $O_2^{\bullet}$ (not shown). In addition, inclusion of citrate failed to promote reactivation of aconitase when H_2O_2 or $O_2^{\bullet}$ production was quenched (not shown). Thus, extended exposure of mitochondria to steady-state concentrations of H_2O_2 or $O_2^{\bullet}$ appears to result in further disassembly of the [4Fe−4S] cluster.

Western blot analysis using antibodies raised against aconitase indicates that degradation of the enzyme occurred following treatment of mitochondria with glucose/glucose oxidase or xanthine/xanthine oxidase for 30 min (Figure 8A). Loss of full-length protein was most evident in mitochondria treated with the $O_2^{\bullet}$ generating system (Figure 8A). The presence of citrate during mitochondrial incubations resulted in greater retention of the full-length protein indicating that citrate protects the enzyme from degradation. As indicated by similar protein distribution visualized by silver staining, universal degradation of protein was not observed. To

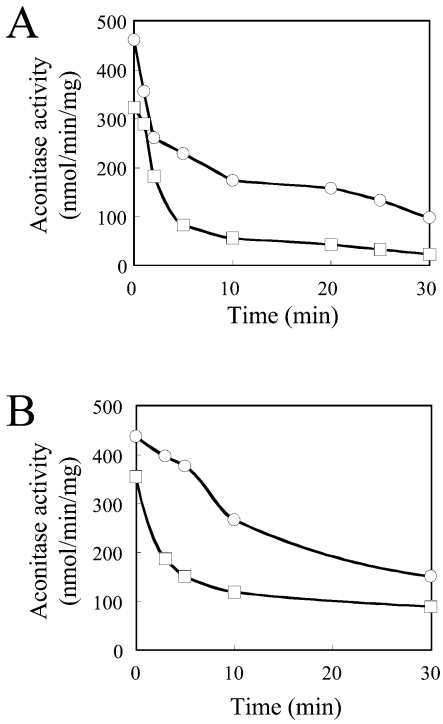

FIGURE 7: Alterations in aconitase activity in response to steady-state production of H_2O_2 or $O_2^{\bullet}$. Panel A: effect of H_2O_2 generating system. Intact mitochondria (0.25 mg/mL) were incubated in the absence (□) or presence (○) of 2.0 mM citrate and treated with a mixture of glucose, glucose oxidase, and catalase to generate H_2O_2 at a steady-state concentration of 100 μM for indicated periods of time (25 °C). Mitochondria were then disrupted, and aconitase activity was determined as described in Materials and Methods. Panel B: effect of $O_2^{\bullet}$ generating system. Intact mitochondria (0.25 mg/mL) were incubated in the absence (□) or presence (○) of 2.0 mM citrate and treated with a mixture of xanthine, xanthine oxidase, and catalase to generate $O_2^{\bullet}$ at a constant rate (2.0 nmol/min/mL) for indicated periods of time (25 °C). Mitochondria were then disrupted, and aconitase activity was determined as described in Materials and Methods.

investigate whether a specific protease might be responsible for aconitase degradation, mitochondria were incubated in the presence of phenylmethylsulfonyl fluoride (PMSF) and *N*-ethylmaleimide (NEM), serine and cysteine protease inhibitors, respectively. Degradation of aconitase was strongly inhibited in the presence of these inhibitors indicating that aconitase becomes susceptible to proteolysis upon oxidative stress (Figure 8A). No change in the level of enzyme inactivation was observed when protease inhibitors were included (Figure 8B). Therefore, aconitase degradation does not contribute to the observed loss in enzyme activity. When ATP was not generated in mitochondria prior to oxidant treatment, Western blot analysis revealed reduced degradation of aconitase (not shown). Taken together, these results indicate that aconitase appears to be degraded by an ATP-stimulated serine/cysteine protease in response to prolonged oxidative stress. It is interesting to note that aconitase exhibits enhanced carbonylation, an index of amino acid oxidation, upon treatment of *Saccharomyces cerevisiae* cells with H_2O_2 (*37*) and as a function of age (*11*). In the current study, mitochondria were treated with a steady-state level of 100 μM H_2O_2 (glucose oxidase or rotenone) or $O_2^{\bullet}$ (xanthine/xanthine oxidase) in the presence of protease inhibitors (PMSF and NEM), and full-length aconitase was immunopurified. Appearance of protein-associated carbonyl groups

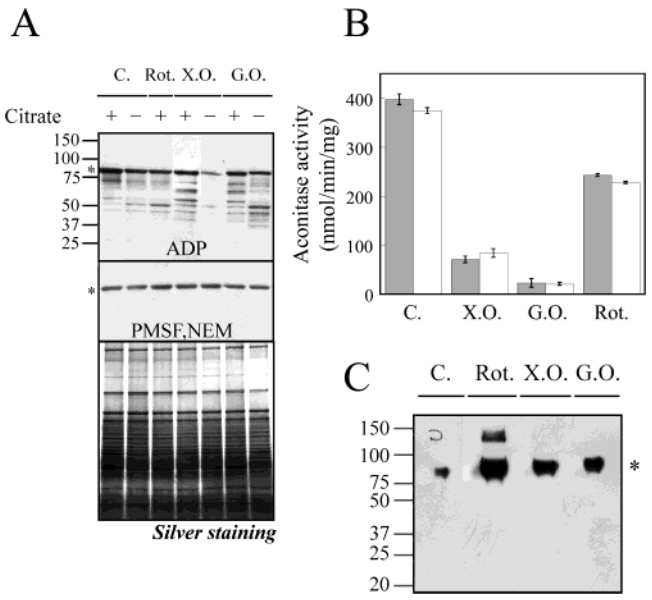

FIGURE 8: Oxidant-induced modification and proteolytic degradation of aconitase. Panel A: effect of oxidants on proteolytic degradation of aconitase. Intact mitochondria (0.25 mg/mL) were incubated (25 °C) in the presence or absence of 2.0 mM citrate, 5.0 mM ADP and treated with glucose/glucose oxidase to yield 100 μM H_2O_2, xanthine/xanthine oxidase to yield 2 nmol/min/mL $O_2^{\bullet}$ or 40 μM rotenone. Mitochondria were also incubated under the same conditions in the presence of 1.0 mM NEM and 5.0 mM PMSF. At 30 min, mitochondria were disrupted, and mitochondrial proteins (10 μg/lane) were resolved by SDS−PAGE (12% gels) and analyzed by Western blot analysis utilizing polyclonal antibodies raised against aconitase as described in Materials and Methods. In addition, gels were silver stained to reveal protein profiles. Blots depicted are representative of three separate experiments. Panel B: effect of oxidants and protease inhibitors on aconitase activity. Aconitase activity in mitochondria incubated with 5.0 mM ADP, 1.0 mM NEM, and 5.0 mM PMSF (gray bars) or in the presence of 5.0 mM ADP without protease inhibitors (white bars) 30 min after exposure of mitochondria to oxidants in the absence of respiratory substrates. Panel C: aconitase was immunopurified in the presence of protease inhibitors (1.0 mM NEM and 5.0 mM PMSF) from mitochondria exposed for 30 min to glucose/glucose oxidase, xanthine/xanthine oxidase, or rotenone. Immunopurified aconitase (2.0 μg of immunopurified protein/lane) was analyzed for the presence of protein-associated carbonyls groups as described in Materials and Methods.

indicates oxidative modification of aconitase (Figure 8C). This was not observed when mitochondria were treated with a bolus of H_2O_2 (100 μM) (not shown). These results are consistent with the progression from reversible aconitase inactivation to cluster disassembly, destabilization of protein structure, and increased proteolytic susceptibility. The fate of aconitase is dependent on the availability of the enzyme's substrate, the source and form of the pro-oxidant species, and the duration of exposure (Scheme 1). In addition, there are a number of enzymes involved in the assembly and repair of Fe−S clusters (*38*, *39*). Oxidant-induced impairment of these processes may contribute to the irreversible nature of aconitase inactivation upon prolonged exposure to certain pro-oxidants.

DISCUSSION

The current study employed intact cardiac mitochondria and various mitochondrial subfractions to characterize the response of mitochondrial aconitase to pro-oxidants. We provide evidence that mitochondrial aconitase undergoes

Scheme 1

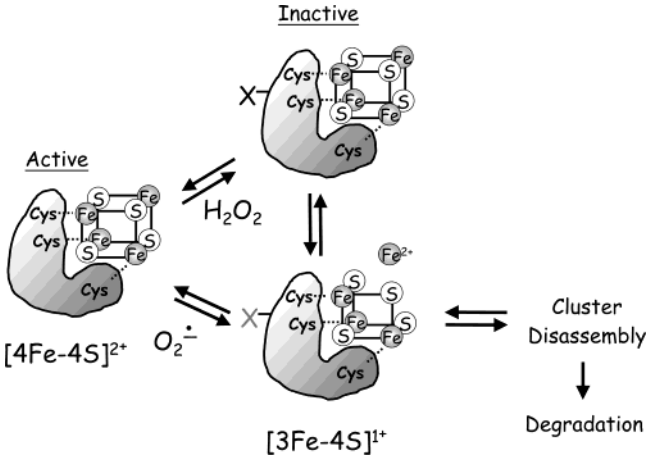

H_2O_2 mediated inactivation. Reactivation begins prior to complete consumption of H_2O_2 and requires the presence of the enzyme's substrate, citrate. H_2O_2 does not exert its inhibitory effects by acting directly on the enzyme, rather inactivation appears to result from interaction(s) between aconitase and a mitochondrial membrane component responsive to H_2O_2. Moreover, as determined utilizing a combination of biochemical and EPR spectroscopic methods, H_2O_2-induced aconitase inactivation precedes release of iron from the $[4Fe-4S]^{2+}$ cluster present in the active site of the enzyme. These observations are consistent with the view that some form of posttranslational modification of aconitase other than release of iron contributes significantly to enzyme inactivation. Depending on the availability of respiratory substrate(s), the mode of pro-oxidant production, the identity of the pro-oxidant species, and the magnitude/duration of the oxidative stress, aconitase can undergo several alterations that determine the metabolic fate of aconitase. These include reversible posttranslational inactivation, release of a labile iron from the $[4Fe-4S]^{2+}$ cluster, disassembly of the [4Fe−4S] cluster, carbonylation, and protein degradation (Scheme 1). Loss of aconitase activity under pathophysiological conditions associated with an increase in free radical production is often regarded as an index of free radical mediated damage (*6*−*8*, *10*, *40*). However, given the reversible nature of the response of aconitase to alterations in redox status, loss in enzyme activity may be indicative of a regulated response to oxidative stress (*14*, *15*). Inhibition of aconitase may serve to reduce the supply of NADH for electron transport, thereby limiting the production of free radical species (*25*).

H_2O_2 has long been considered to exert effects on protein function through direct interactions and/or through the formation of more potent oxidants via Fenton chemistry (*41*). Emerging evidence indicates that H_2O_2 can also alter protein function through the activation of signaling cascades (*27*, *42*−*46*). We have provided evidence that mitochondrial aconitase (m-aconitase) is not directly sensitive to H_2O_2 under the conditions of our experiments. A mitochondrial membrane component(s) is required for H_2O_2-mediated inactivation. Previously, H_2O_2 has been found to stimulate the conversion of cytosolic aconitase (c-aconitase) to IRP1 through loss of its [4Fe−4S] cluster. This does not involve the direct interaction of H_2O_2 with the [4Fe−4S] cluster but proceeds via an unknown signaling pathway involving a

membrane-bound component (*47*−*49*). A number of physiologically relevant sulfhydryl modifications that alter protein function have been shown to be reversible by enzymatic processes (*44*, *45*, *50*, *51*). These include disulfide bonds, mixed disulfides with glutathione, sulfenic acid, and more recently, sulfinic acid. An interesting example involves Yap1, a transcription factor that regulates hydroperoxide homeostasis in *S. cerevisiae*. Gpx3, a thiol peroxidase, acts as a H_2O_2 sensor that promotes the formation of a Yap1 intramolecular disulfide bond leading to Yap1 activation. Thioredoxin inactivates this pathway by reducing disulfides within Gpx3 and Yap1 (*52*, *53*). It is well-known that m-aconitase contains a highly reactive cysteine residue (*12*, *13*). Reaction of this residue with various sulfhydryl reagents causes inactivation of the enzyme (*36*, *54*, *55*). It is therefore possible that H_2O_2 inactivates m-aconitase by inducing oxidation of this cysteine residue through the action(s) of a membrane component. An alternative possibility is H_2O_2-induced phosphorylation of m-aconitase. Phosphorylation is known to influence the ease with which the conversion between c-aconitase and IRP1 can proceed (*56*−*58*).

It has previously been shown that exposure of m- or c-aconitase to H_2O_2 or $O_2^{\bullet}$ results in enzyme inactivation and the appearance of an EPR signal corresponding to the $[3Fe-4S]^{1+}$ cluster of the enzyme (*1*−*4*, *59*). It has therefore been widely accepted that release of the labile iron from the [4Fe−4S] cluster is responsible for enzyme inactivation upon exposure to various pro-oxidants (*5*). In this study, treatment of cardiac mitochondria with H_2O_2 in the presence of citrate clearly results in the formation of the $[3Fe-4S]^{1+}$ cluster of aconitase. However, the relative level and time-dependent appearance of this form of the enzyme does not reflect the magnitude of enzyme inactivation. This is evident upon comparison of the distribution of various forms of aconitase as judged by IEF gel electrophoresis and the relative level of enzyme inactivation. In addition, enzyme inactivation preceded the appearance of an EPR signal corresponding to the $[3Fe-4S]^{1+}$ cluster. Furthermore, the maximum intensity of the signal was significantly greater in mitochondria treated with rotenone relative to H_2O_2, despite the fact that the magnitude of aconitase inactivation was less. Therefore, while it is clear that release of a labile iron occurs in cardiac mitochondria treated with H_2O_2 in the presence of citrate, this does not appear to be the primary event responsible for loss of aconitase activity. Reactivation of aconitase in H_2O_2 treated mitochondria occurs only in the presence of citrate under the conditions of our experiments. Citrate may therefore facilitate the reinsertion of iron into the cluster and may participate in the reversal of the posttranslational modification(s) responsible for enzyme inactivation (*12*).

Exposure of cardiac mitochondria to enzymatic systems that produce steady-state levels of H_2O_2 or $O_2^{\bullet}$ results in disassembly of the iron−sulfur cluster of aconitase, oxidation of amino acid side chains (carbonylation), and proteolytic degradation. It has recently been reported that treatment of Arabidopsis cells with H_2O_2 resulted in the induction of a mitochondrial protease believed to be responsible for the degradation of oxidatively damaged protein (*60*). Moreover, purified aconitase subjected to extensive oxidative modifications by exposure to millimolar concentrations of H_2O_2 exhibited enhanced susceptibility to proteolysis by purified Lon protease (*26*). Under the conditions of our experiments, degradation of aconitase appears stimulated by ATP and is inhibited by PMSF and NEM, properties consistent with proteolysis by the Lon protease. Rotenone induced a greater level of aconitase carbonylation and a lower level of cluster disassembly and proteolytic degradation than mitochondria incubated with glucose/glucose oxidase (H_2O_2) or xanthine/xanthine oxidase ($O_2^{\bullet}$). It therefore appears that cluster disassembly and destabilization of protein structure may play a greater role in increasing proteolytic susceptibility than oxidation of amino acid chains. Citrate, which binds to the [4Fe−4S] cluster of the enzyme, protects from degradation providing further support for the importance of cluster destabilization in this process. The greater level of carbonylation of aconitase upon rotenone-induced $O_2^{\bullet}$ formation indicates that the location of pro-oxidant generation is important for protein amino acid oxidation. Cluster disassembly in the case of pro-oxidant generating systems, glucose/glucose oxidase (H_2O_2) or xanthine/xanthine oxidase ($O_2^{\bullet}$), is inferred by the lack of an EPR signal and the inability to reactivate aconitase in the presence of citrate when pro-oxidant generation is quenched and proteolysis is inhibited. NADH is required for electron transport and rotenone-induced $O_2^{\bullet}$ generation. The lower level of aconitase [4Fe−4S] cluster disassembly in rotenone treated mitochondria, as judged by the intensity of the EPR detectable $[3Fe-4S]^{1+}$ cluster, is therefore likely due to oxidant-induced reduction in the supply of NADH. Clearly, the mode of inactivation and long-term fate of aconitase is dependent on the availability of the enzyme's substrate, the nature of the pro-oxidant species, and the duration of exposure (Scheme 1).

The significance of the current study is the discovery that the activity of mitochondrial aconitase is modulated by a membrane component that is responsive to alterations in H_2O_2 concentration. Additionally, evidence indicates that inactivation involves posttranslational modification of aconitase and does not necessarily require release of iron from the [4Fe−4S] cluster of aconitase. However, if the oxidative stress is of sufficient magnitude and duration to promote cluster disassembly and aconitase carbonylation, inactive aconitase is degraded by an ATP-dependent mitochondrial protease, potentially Lon. Future studies that seek to identify the mechanism(s) and mitochondrial components responsible for aconitase inactivation and reactivation are necessary to delineate the physiological relevance of aconitase inactivation during numerous degenerative conditions associated with oxidative stress.

ACKNOWLEDGMENT

We thank M. Claire Kennedy for helpful discussions.

REFERENCES

1. Brazzolotto, X., Gaillard, J., Pantopoulos, K., Hentze, M. W., and Moulis, J. M. (1999) *J. Biol. Chem. 274*, 21625−21630.
2. Vasquez-Vivar, J., Kalyanaraman, B., and Kennedy, M. C. (2000) *J. Biol. Chem. 275*, 14064−14069.
3. Verniquet, F., Gaillard, J., Neuburger, M., and Douce, R. (1991) *Biochem. J. 276*, 643−648.
4. Beinert, H., Kennedy, M. C., and Stout, C. D. (1996) *Chem. Rev. 96*, 2335−2374.
5. Gardner, P. R. (2002) *Methods Enzymol. 349*, 9−23.
6. Adam-Vizi, V. (2003) *J. Neurochem. 85 Suppl 2*, 3.

7. Schapira, A. H. (1999) *Biochim. Biophys. Acta 1410*, 159−170.
8. Sipos, I., Tretter, L., and Adam-Vizi, V. (2003) *J. Neurochem. 84*, 112−118.
9. Sadek, H. A., Humphries, K. M., Szweda, P. A., and Szweda, L. I. (2002) *Arch. Biochem. Biophys. 406*, 222−228.
10. Tretter, L., and Adam-Vizi, V. (2000) *J. Neurosci. 20*, 8972−8979.
11. Yan, L. J., Levine, R. L., and Sohal, R. S. (1997) *Proc. Natl. Acad. Sci. U.S.A. 94*, 11168−11172.
12. Kennedy, M. C., Emptage, M. H., Dreyer, J. L., and Beinert, H. (1983) *J. Biol. Chem. 258*, 11098−11105.
13. Emptage, M. H., Dreyers, J. L., Kennedy, M. C., and Beinert, H. (1983) *J. Biol. Chem. 258*, 11106−11111.
14. Gardner, P. R. (1997) *Biosci. Rep. 17*, 33−42.
15. Gardner, P. R., Raineri, I., Epstein, L. B., and White, C. W. (1995) *J. Biol. Chem. 270*, 13399−13405.
16. Beinert, H., and Kennedy, M. C. (1993) *FASEB J. 7*, 1442−1449.
17. Beinert, H., and Kiley, P. J. (1999) *Curr. Opin. Chem. Biol. 3*, 152−157.
18. Theil, E. C., and Eisenstein, R. S. (2000) *J. Biol. Chem. 275*, 40659−40662.
19. Eisenstein, R. S., and Blemings, K. P. (1998) *J. Nutr. 128*, 2295−2298.
20. Eisenstein, R. S. (2000) *Annu. Rev. Nutr. 20*, 627−662.
21. Haile, D. J., Rouault, T. A., Harford, J. B., Kennedy, M. C., Blondin, G. A., Beinert, H., and Klausner, R. D. (1992) *Proc. Natl. Acad. Sci. U.S.A. 89*, 11735−11739.
22. Turrens, J. F., and Boveris, A. (1980) *Biochem. J. 191*, 421−427.
23. Chance, B., Sies, H., and Boveris, A. (1979) *Physiol. Rev. 59*, 527−605.
24. Cadenas, E., and Davies, K. J. (2000) *Free Radical Biol. Med. 29*, 222−230.
25. Skulachev, V. P. (1997) *Biosci. Rep. 17*, 347−366.
26. Bota, D. A., and Davies, K. J. (2002) *Nat. Cell Biol. 4*, 674−680.
27. Nulton-Persson, A. C., and Szweda, L. I. (2001) *J. Biol. Chem. 276*, 23357−23361.
28. Kuzela, S., and Goldberg, A. L. (1994) *Methods Enzymol. 244*, 376−383.
29. Mueller, S., and Pantopoulos, K. (2002) *Methods Enzymol. 348*, 324−337.
30. Esposti, M. D., Hatzinisiriou, I., McLennan, H., and Ralph, S. (1999) *J. Biol. Chem. 274*, 29831−29837.
31. Han, D., Antunes, F., Daneri, F., and Cadenas, E. (2002) *Methods Enzymol. 349*, 271−280.
32. Des Rosiers, C., Di Donato, L., Comte, B., Laplante, A., Marcoux, C., David, F., Fernandez, C. A., and Brunengraber, H. (1995) *J. Biol. Chem. 270*, 10027−10036.
33. Lill, R., and Kispal, G. (2000) *Trends Biochem. Sci. 25*, 352−356.
34. Lill, R., Diekert, K., Kaut, A., Lange, H., Pelzer, W., Prohl, C., and Kispal, G. (1999) *Biol. Chem. 380*, 1157−1166.
35. Muhlenhoff, U., and Lill, R. (2000) *Biochim. Biophys. Acta 1459*, 370−382.
36. Ramsay, R. R., Dreyer, J. L., Schloss, J. V., Jackson, R. H., Coles, C. J., Beinert, H., Cleland, W. W., and Singer, T. P. (1981) *Biochemistry 20*, 7476−7482.
37. Cabiscol, E., Piulats, E., Echave, P., Herrero, E., and Ros, J. (2000) *J. Biol. Chem. 275*, 27393−27398.
38. Li, J., Kogan, M., Knight, S. A., Pain, D., and Dancis, A. (1999) *J. Biol. Chem. 274*, 33025−33034.
39. Gerber, J., and Lill, R. (2002) *Mitochondrion 2*, 71−86.
40. Li, Q. Y., Pedersen, C., Day, B. J., and Patel, M. (2001) *J. Neurochem. 78*, 746−755.
41. Halliwell, B., and Gutteridge, J. M. (1990) *Methods Enzymol. 186*, 1−85.
42. Finkel, T. (1998) *Curr. Opin. Cell Biol. 10*, 248−253.
43. Nulton-Persson, A. C., Starke, D. W., Mieyal, J. J., and Szweda, L. I. (2003) *Biochemistry 42*, 4235−4242.
44. Starke, D. W., Chock, P. B., and Mieyal, J. J. (2003) *J. Biol. Chem. 278*, 14607−14613.
45. Rhee, S. G., Bae, Y. S., Lee, S. R., and Kwon, J. (2000) *Sci. STKE 2000*, PE1.
46. Qin, S., and Chock, P. B. (2003) *Biochemistry 42*, 2995−3003.
47. Pantopoulos, K., and Hentze, M. W. (1995) *EMBO J. 14*, 2917−2924.
48. Pantopoulos, K., and Hentze, M. W. (1998) *Proc. Natl. Acad. Sci. U.S.A. 95*, 10559−10563.
49. Pantopoulos, K., Mueller, S., Atzberger, A., Ansorge, W., Stremmel, W., and Hentze, M. W. (1997) *J. Biol. Chem. 272*, 9802−9808.
50. Woo, H. A., Chae, H. Z., Hwang, S. C., Yang, K. S., Kang, S. W., Kim, K., and Rhee, S. G. (2003) *Science 300*, 653−656.
51. Kamata, H., and Hirata, H. (1999) *Cell Signal 11*, 1−14.
52. Delaunay, A., Isnard, A. D., and Toledano, M. B. (2000) *EMBO J. 19*, 5157−5166.
53. Delaunay, A., Pflieger, D., Barrault, M. B., Vinh, J., and Toledano, M. B. (2002) *Cell 111*, 471−481.
54. Kennedy, M. C., and Beinert, H. (1988) *J. Biol. Chem. 263*, 8194−8198.
55. Kennedy, M. C., Spoto, G., Emptage, M. H., and Beinert, H. (1988) *J. Biol. Chem. 263*, 8190−8193.
56. Eisenstein, R. S., Tuazon, P. T., Schalinske, K. L., Anderson, S. A., and Traugh, J. A. (1993) *J. Biol. Chem. 268*, 27363−27370.
57. Schalinske, K. L., Anderson, S. A., Tuazon, P. T., Chen, O. S., Kennedy, M. C., and Eisenstein, R. S. (1997) *Biochemistry 36*, 3950−3958.
58. Schalinske, K. L., and Eisenstein, R. S. (1996) *J. Biol. Chem. 271*, 7168−7176.
59. Brown, N. M., Kennedy, M. C., Antholine, W. E., Eisenstein, R. S., and Walden, W. E. (2002) *J. Biol. Chem. 277*, 7246−7254.
60. Sweetlove, L. J., Heazlewood, J. L., Herald, V., Holtzapffel, R., Day, D. A., Leaver, C. J., and Millar, A. H. (2002) *Plant J. 32*, 891−904.

BI0353979